

- under statistical conditions [K. A. Boering and J. I. Brauman, *J. Chem. Phys.* **97**, 5439 (1992)].
32. J. March, *Advanced Organic Chemistry* (Wiley, New York, ed. 4, 1992).
  33. R. A. Marcus, *J. Phys. Chem. A* **101**, 4072 (1997).
  34. A. Streitwieser, *Solvolytic Displacement Reactions* (McGraw-Hill, New York, 1962).
  35. Accurate measurement of slow rate constants is difficult because side reactions of small amounts of impurities can be faster than the reaction of interest. For example, 0.1% of an impurity that reacts on every collision occurs at the same rate as a reaction being studied that has an efficiency of  $10^{-3}$ .
  36.  $\Delta E_{\text{O}}^{\ddagger}$  is a hypothetical quantity representing the activation energy when the exothermicity,  $\Delta E^{\circ}$ , is zero.
  37. J. R. Murdoch, *J. Am. Chem. Soc.* **94**, 4410 (1972).
  38. R. A. Marcus, *Annu. Rev. Phys. Chem.* **15**, 155 (1964).
  39. J. A. Dodd and J. I. Brauman, *J. Am. Chem. Soc.* **106**, 5356 (1984).
  40. B. D. Wladkowski and J. I. Brauman, *J. Phys. Chem.* **97**, 13158 (1993).
  41. S. Wolfe, D. J. Mitchell, H. B. Schlegel, *J. Am. Chem. Soc.* **103**, 7692 (1981).
  42. ———, *ibid.*, p. 7694.
  43. M. J. Pellerite and J. I. Brauman, *ibid.* **102**, 5993 (1980).
  44. ———, *ibid.* **105**, 2672 (1983).
  45. F. Jensen, *Chem. Phys. Lett.* **196**, 368 (1992).
  46. H. van der Wel *et al.*, *J. Am. Chem. Soc.* **109**, 5823 (1987).
  47. S. L. Craig and C. K. Regan, unpublished results.
  48. Honig, for example, has shown that the Born solvation model can provide accurate solvation energies for simple ions. It has also successfully been applied to more complex molecular systems in the form of the Poisson-Boltzmann equation [B. Honig and A. Nicholls, *Science* **268**, 1144 (1995)]. Truhlar has shown that a similar approach can give reasonable agreement with the experimental reaction barrier in a model  $S_{\text{N}}2$  reaction [S. C. Tucker and D. G. Truhlar, *Chem. Phys. Lett.* **157**, 164 (1989)].
  49. J. P. Bergsma *et al.*, *J. Chem. Phys.* **86**, 1356 (1987).
  50. D. K. Bohme and A. B. Raksit, *J. Am. Chem. Soc.* **106**, 3447 (1984).
  51. P. M. Hierl, A. F. Ahrens, M. J. Henchman, A. A. Viggiano, J. F. Paulson, *Faraday Discuss. Chem. Soc.* **85**, 37 (1988).
  52. A. Gonzalez-Lafont and D. G. Truhlar, in *Chemical Reactions in Clusters*, E. R. Bernstein, Ed. (Oxford Univ. Press, New York, 1996), pp. 3–39.
  53. M. Arshadi, R. R. Yamdagni, P. Kebarle, *J. Phys. Chem.* **74**, 1475 (1970).
  54. R. C. Dunbar *et al.*, *J. Am. Chem. Soc.* **117**, 12819 (1995).
  55. K. Morokuma, *ibid.* **104**, 3733 (1982).
  56. X. G. Zhao *et al.*, *J. Chem. Phys.* **97**, 6369 (1992).
  57. S. C. Tucker and D. G. Truhlar, *J. Am. Chem. Soc.* **112**, 3347 (1990).
  58. S. E. Barlow, J. M. V. Doren, V. M. Bierbaum, *ibid.* **110**, 7240 (1988).
  59. D. Bohme, in *Ionic Processes in the Gas Phase*, M. A. A. Ferreira, Ed. (Reidel, Dordrecht, 1984).
  60. W.-P. Hu and D. G. Truhlar, *J. Am. Chem. Soc.* **116**, 7797 (1994).
  61. S. L. Craig and J. I. Brauman, *ibid.* **118**, 6786 (1996).
  62. S. Baer *et al.*, *ibid.* **111**, 4097 (1989).
  63. Supported by NSF and fellowships from NSF (to S.L.C. and M. L.C.), the American Chemical Society Division of Organic Chemistry (to S.L.C. and M.L.C.), and the General Electric Fund (C.K.R.).

# Chemical Dynamics in Proteins: The Photoisomerization of Retinal in Bacteriorhodopsin

Feng Gai,\* K. C. Hasson,† J. Cooper McDonald, Philip A. Anfinrud‡

Chemical dynamics in proteins are discussed, with bacteriorhodopsin serving as a model system. Ultrafast time-resolved methods used to probe the chemical dynamics of retinal photoisomerization in bacteriorhodopsin are discussed, along with future prospects for ultrafast time-resolved crystallography. The photoisomerization of retinal in bacteriorhodopsin is far more selective and efficient than in solution, the origins of which are discussed in the context of a three-state model for the photoisomerization reaction coordinate. The chemical dynamics are complex, with the excited-state relaxation exhibiting a multiexponential decay with well-defined rate constants. Possible origins for the two major components are also discussed.

The chemistry of life as we know it requires a myriad of enzyme-catalyzed reactions, all of which take place in the condensed phase. These reactions proceed with remarkable efficiency and selectivity, the likes of which are rarely duplicated in non-biological systems. The key difference lies in the solvent. In biological systems, the “solvent” surrounding the active site is often a highly organized protein whose architecture influences the chemical behavior at the active center. Moreover, that architec-

ture can provide docking sites to house intermediates involved in the reaction and can create species-selective passageways between the active site and the surrounding solution. The structure of a protein, therefore, tailors its function. Static structures determined at atomic resolution can reveal the relative proximity and orientation of functional groups and can help to rationalize a protein’s chemical behavior; however, to be able to predict its chemical behavior, we must understand the influence of its architecture on its chemical dynamics. This insight may allow the design of new protein sequences that fold into target structures and execute a designed function and may also help to assess the function of proteins that will be discovered as a consequence of sequencing the human genome. Generating this level of understanding will require contributions from molecular dynamics, quan-

tum mechanics, molecular biology, and time-resolved spectroscopy and crystallography. The rapid pace of advances among these methods is pushing this goal ever closer to reality.

In the context of this article, “chemical dynamics” relates to the pathway by which chemical bonds are broken and formed. The breaking and making of bonds renders the process “chemical,” and the term “dynamics” hints at the fact that the dominant outcome corresponds to the fastest of several possible pathways. A detailed understanding of chemical dynamics requires knowledge of both electronic and nuclear motion along the predominant reaction pathway and is often summarized in the form of a simple potential energy surface that depicts the putative reaction pathway as well as its associated dynamics.

Whether occurring within a protein or in the gas phase, chemical transformations proceed on the femtosecond time scale. Consequently, direct investigations into chemical dynamics require methods that provide femtosecond time resolution. Currently, all such methods are pump-probe techniques, where an ultrashort pulse of light excites a chromophore and triggers the process to be investigated. The pump-probe approach, therefore, constrains the experimental study of chemical dynamics in proteins to photobiological systems (such as the rhodopsins, the photosynthetic reaction center, photoactive yellow protein, and phytochrome) or to proteins that can be optically triggered (for example, the photodetachment of ligands from ligand-binding heme proteins). Nevertheless, incisive experimental characterization of chemical dynamics in a small number of photoactive proteins should provide sufficient constraints with which to test and refine general theoretical models of chemical dynamics in proteins.

The authors are in the Department of Chemistry and Chemical Biology, Harvard University, 12 Oxford Street, Cambridge, MA 02138, USA.

\*Present address: Los Alamos National Laboratory, CST-4, MS J586, Los Alamos, NM 87545, USA.

†Present address: Magnetic Imaging Technologies, 2500 Meridian Parkway, Suite 175, Durham, NC 27713, USA.

‡To whom correspondence should be addressed. E-mail: anfinrud@chemistry.harvard.edu

The spectrum of a chromophore is often sensitive to its electronic state, its conformation, and its surrounding environment, thereby providing a spectroscopic handle for probing its chemical dynamics. Suitable spectroscopic methods include time-resolved fluorescence, absorbance, and resonance Raman spectroscopy. Whereas fluorescence emission spectroscopy probes molecules in their excited electronic state, absorbance spectroscopy is sensitive to all species along the reaction pathway. The lack of specificity in the transient absorbance spectrum can become a problem when the features are broad and overlapping; however, this complication can be partially overcome by probing the transient absorbance over a broad spectral range with high sensitivity and by using multiple-pulse techniques. Time-resolved resonance Raman spectroscopy reveals vibrational features and indirectly provides coveted structural information; however, these vibrational features are often unresolved when the time resolution is made sufficiently short to probe chemical dynamics.

Unfortunately, the intermediates observed in time-resolved optical spectra are not readily assigned to the molecular structures that give rise to those features. Studies of chemical dynamics would benefit greatly from methods that can determine the molecular structure of transient intermediates. Significant progress is being made in the area of time-resolved x-ray crystallography: the structures of photolyzed carbon monoxymyoglobin and photoactive yellow protein were recently determined with about 10-ns time resolution (1). The infrastructure required to extend the time resolution to approximately 100 ps is being put into place at the European Synchrotron and Radiation Facility (ESRF), with the first picosecond time-resolved x-ray crystallography experiments scheduled for early 1998 (2). In principle, these methods could be extended to the femtosecond time domain by the production of x-rays with an ultrashort electron pulse of several billion electron volts generated in a linear accelerator. The x-ray brilliance (3) and pulse duration achievable with such a linear accelerator should be sufficient to determine protein structures with subpicosecond time resolution. Other approaches for generating subpicosecond x-ray pulses have been reported (4), but they lack the x-ray brilliance needed to pursue time-resolved protein crystallography. Because the potential of femtosecond time-resolved protein crystallography has not yet been realized, the most incisive information regarding chemical dynamics in proteins currently comes from ultrafast time-resolved optical approaches.

To illustrate what can be learned about

chemical dynamics in proteins, we direct our attention to the photoisomerization of retinal, a process that has been studied in both solution and proteins. A comparison of the outcome in solution and in bacteriorhodopsin (bR) is particularly instructive because it reveals the extent to which a protein can influence both the efficiency and selectivity of a photochemical reaction. Our focus on bR is also motivated by potential applications in optical computing (5), by the availability of high-resolution structures from both electron (6) and x-ray crystallography (7), by the ability to probe chemical dynamics in site-directed bR mutants (8, 9) as well as bR reconstituted with chemically modified retinals (10, 11), and by the ability to probe chemical dynamics in related retinal proteins such as rhodopsin and halorhodopsin (12).

### Bacteriorhodopsin

Bacteriorhodopsin is a 26-kD protein found in the purple membrane of *Halobacterium halobium*, an archaeobacterium that thrives in the harsh environment of salt marshes (13). Upon illumination with visible light, this protein develops a proton-motive force, which drives the synthesis of adenosine triphosphate (ATP) (14). The light-absorbing chromophore responsible for this activity is a retinal molecule (15) (Fig. 1) that is covalently attached to the protein through a protonated Schiff base linkage to Lys<sup>216</sup> (16). Retinal photoisomerizes from its all-*trans* to its 13-*cis* form (17) and triggers the translocation of one proton from the cytoplasmic side of the membrane to the extracellular side (18). After executing this function, the 13-*cis* form spontaneously reverts back to all-*trans* retinal, and the photocycle is repeated.

In order for the bacterium to engage in photosynthesis with reasonable efficiency, the absorbance spectrum of the chromophore has to overlap with the solar irradiance, which is peaked near 500 nm. When linked to an unprotonated Schiff base in methanol solution, all-*trans* retinal has an absorbance maximum near 360 nm (19). When the Schiff base is protonated, the absorbance shifts to about 450 nm (19). When bound to bR through a protonated Schiff base linkage, the absorbance is further shifted to about 570 nm. This "opsin" shift (20) optimizes the retinal absorbance for carrying out photosynthesis. The choice of a conjugated polyene as a chromophore could, in principle, compromise selectivity: the protonated Schiff base of retinal possesses six conjugated double bonds and, therefore, provides multiple centers for photoisomerization. Indeed, the photoisomerization of retinal in methanol solution is neither very se-

lective nor efficient. After photoexcitation, the unprotonated Schiff base of all-*trans* retinal can isomerize to form 9-*cis*, 11-*cis*, or 13-*cis* retinal, with efficiencies of 0, 6, and 6%, respectively (19). When the Schiff base is protonated, the respective isomerization efficiencies become 2, 14, and 1% (19). In stark contrast, the protonated Schiff base of retinal in bR selectively photoisomerizes to the 13-*cis* form with an efficiency of 64% (21). Indeed, it has been suggested that the protein plays a catalytic role in the photoisomerization of retinal (8, 22). The propensity to photoisomerize is intrinsic to the retinal; however, the architecture of the protein surrounding the retinal in bR influences that photoreaction to make it both highly selective and efficient. How the protein modifies the chemical dynamics of this photoisomerization is the primary focus of this article. The mechanism by which this photoisomerization event leads to unidirectional proton transport has been reviewed elsewhere (23).

### Photoisomerization Reaction Coordinate

We seek a model for the photoisomerization of retinal in bR that can account for both its high selectivity and efficiency. We first consider the nature of the thermal isomerization coordinate along the ground electronic state. Photocalorimetry studies showed that the 13-*cis* form is about 40 to 50 kJ mol<sup>-1</sup> higher in enthalpy than the all-*trans* form (24, 25), thereby storing sufficient energy to pump one proton across the cell membrane and drive retinal back to its all-*trans* form. Thermal isomerization from 13-*cis* back to all-*trans* retinal is fast, occurring at a rate of 100 s<sup>-1</sup> at 20°C (26). Evidently, the protein surrounding retinal not only destabilizes its

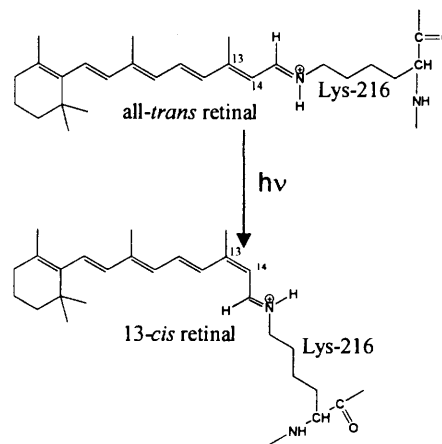


**Fig. 1.** Retinal with a protonated Schiff base. In bR, the retinal is housed within the hydrophobic interior of a seven-helix bundle and is covalently linked to Lys<sup>216</sup>. Upon absorbing a photon, the retinal isomerizes around the C<sub>13</sub>-C<sub>14</sub> bond.

13-*cis* conformation (27) but also catalyzes the rate-limiting return to its all-*trans* conformation, thereby attaining faster photocycling. In contrast, 13-*cis* retinal in solution is quite stable, and thermal isomerization to all-*trans* retinal is extremely slow. The proton-pumping cycle in bR is, of course, a light-activated process, so we now turn our attention to the excited electronic state from which isomerization is launched.

The first picosecond time-resolved absorbance spectra of bR, recorded more than two decades ago, showed that the primary step in the photoreaction occurs in less than 6 ps, the time resolution of the measurement (28). Numerous resonance Ra-

man studies have probed the conformational and vibrational states of the primary photoproduct (29). Like the first time-resolved absorbance study, the time resolution of resonance Raman techniques was not sufficient to resolve the chemical dynamics of bR. About one decade ago, three ultrafast absorbance studies probed the chemical dynamics directly and found that a photoreaction occurs with a 0.5-ps time constant (30–32). Furthermore, it was suggested (31, 32) that the excited-state potential energy surface is “reactive” along the isomerization coordinate, thereby driving the photoexcited all-*trans* retinal toward the 13-*cis* photoproduct along a barrierless path; that is, torsional strain appears promptly in the C<sub>13</sub>-C<sub>14</sub> bond when retinal is promoted into its excited electronic state.

Several conditions have to be met for this model (Fig. 2A) to apply. First, the fluorescence lifetime should be quite short and largely temperature independent; however, the fluorescence lifetime of bR increases from about 0.5 ps at room temperature to 40 ps at 90 K and 60 ps at 77 K (33), a trend that is consistent with a barrier of 4 kJ mol<sup>-1</sup> that must be surmounted before photoisomerization can occur. Second, the fluorescence emission spectrum should rapidly shift to lower energies as the conformation of the retinal progresses along the isomerization coordinate toward the 13-*cis* configuration; however, time-resolved absorbance spectra

suggest that the stimulated emission spectrum develops in about 30 fs (34) and remains stable to beyond 1 ps (35). Because the excited-state spectrum develops in a time far too short for retinal to isomerize, the conformation of photoexcited bR (bR\*) must be much nearer the structure of all-*trans* than 13-*cis* retinal. Evidently, the excited state accessed by one-photon absorption is characterized by a shallow well in the excited-state isomerization coordinate, suggesting that the excited-state potential energy surface is more complex than that depicted in the two-state model.

Before discussing an alternative model for photoisomerization, further elaboration of the time-resolved absorbance spectra is warranted. The stimulated emission contribution to the spectra (Fig. 3) does not match that expected from the fluorescence emission spectrum, despite the fact that they are trivially related to each other. Their peak positions are significantly shifted, suggesting that part of the stimulated emission spectrum in Fig. 3 is canceled by an overlapping excited-state absorbance (35, 36). This suggestion was supported by other parallel studies (10, 37) and was subsequently confirmed by ultrafast three-pulse pump-dump-probe spectroscopy (38), a technique developed to characterize overlapping features in time-resolved absorbance spectra.

A simple three-state model of the potential energy surface (Fig. 2B) has been developed on both theoretical (39) and experimental grounds (35, 36). The three states correspond to the ground state, the excited state accessed by one-photon absorption, and a second “reactive” excited state that is accessed by an adiabatic transition from the first excited state. According to this model, the photoreaction in the all-*trans*→13-*cis* direction encounters a small barrier, leading to a temperature-dependent fluorescence lifetime, as is observed (33). Moreover, the stimulated emission spectrum should be stable over time, as is observed (35, 36). In contrast, the photoreaction in the 13-*cis*→all-*trans* direction is predicted to be barrierless. To test this prediction, a three-pulse experiment was designed in which the first optical pulse produced 13-*cis* retinal, the second pulse photoexcited the 13-*cis* retinal, and a third pulse probed the time-dependent population of the photoexcited state. The excited-state relaxation times for both photoexcited all-*trans* (denoted bR\*) and 13-*cis* (denoted K\*) retinal were determined (Fig. 4). The photoreaction after excitation of 13-*cis* retinal is significantly faster than that of all-*trans*, indicating that the process on the 13-*cis* side is essentially barrierless, as predicted by the three-state model. Evidently, the chemical dynamics

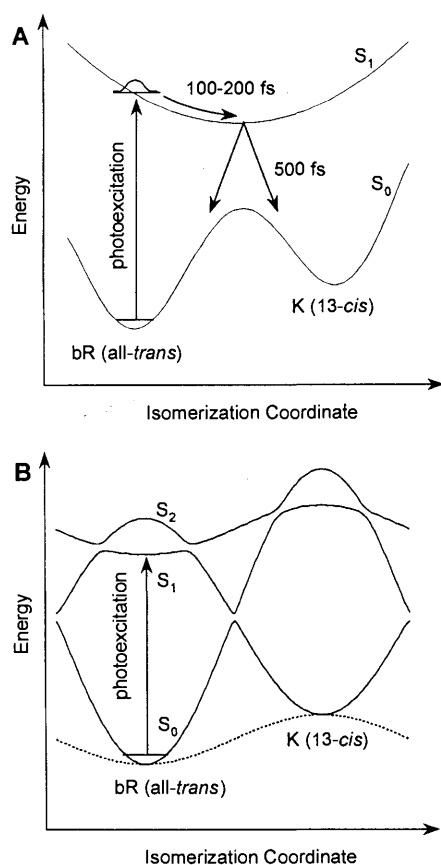


**Fig. 2.** Proposed reaction coordinates for the photoisomerization of retinal in bR: (A) Two-state model ( $S_0$ ,  $S_1$ ). Photoexcitation to a repulsive potential drives the conformation toward the other isomer. The excited-state potential is similar on the *trans* and *cis* sides of the isomerization coordinate, implying that their excited-state dynamics are similar as well. (B) Three-state model ( $S_0$ ,  $S_1$ ,  $S_2$ ). Photoexcitation promotes all-*trans* retinal to a shallow minimum in the excited-state potential. A small barrier must be surmounted for isomerization to occur. In contrast, the photoreaction on the 13-*cis* side is barrierless, owing to the energy bias that elevates the 13-*cis* relative to the all-*trans* isomer. [Adapted from figures 1 and 6 of (35); copyright 1996, U.S. National Academy of Sciences]

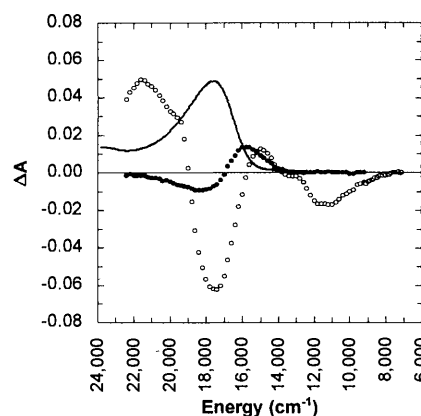


**Fig. 3.** Time-resolved absorbance spectra of bR recorded (50) at 0.316 ps (open circles) and 31.6 ps (filled circles). In the 0.316-ps spectrum, the negative-going feature centered at 17,600 cm<sup>-1</sup> corresponds to photon-induced depletion of the ground-state absorbance; the negative-going feature peaked near 11,000 cm<sup>-1</sup> corresponds to stimulated emission. Positive-going features correspond to excited-state or photoproduct absorbances. The 31.6-ps spectrum consists only of depleted ground-state and photoproduct absorbances. For comparison, a scaled equilibrium absorbance spectrum is shown (thick line). [Adapted from figure 2 of (35); copyright 1996, U.S. National Academy of Sciences]

for the reverse photoisomerization in bR are similar to that for the barrierless 11-*cis* to all-*trans* isomerization in the visual pigment rhodopsin (40).

### Origins of Selectivity and Efficiency

Photoisomerization selectivity and efficiency are separable issues. To rationalize selectivity, note that the isomerization coordinate shown in Fig. 2B is a cut from the multidimensional potential energy surface that governs nuclear motion along all coordinates. Corresponding cuts along the 7-, 9-, and 11-*cis* directions should be qualitatively similar because each involves isomerization about a double bond. The barrier to isomerization along each of these cuts is different, however, with the protein regulating the height of each barrier. The barrier along the all-*trans*→13-*cis* direction need only be about 7 kJ mol<sup>-1</sup> lower than the others to achieve 100:1 selectivity in favor of that pathway. Therefore, the relative rates for surmounting the barriers are much more important than the absolute rates, and the rate of surmounting the barrier need not be ultrafast for the reaction to be selective.

Photoisomerization efficiency is dictated by competition between the rate of radiationless transitions back to the ground electronic state and the speed of nuclear rearrangement along the isomerization coordinate. The rate of radiationless transitions is exponentially dependent on the energy gap  $\Delta E$  between the excited and ground states [ $\propto \exp(-\Delta E)$ ] (41) and becomes quite fast as the reaction approaches the midpoint along the isomerization coordinate. When a radiationless transition occurs while on the all-*trans* side of the isomerization coordinate (Fig. 2B), the retinal will likely remain in its all-*trans* form, and the photon energy will be dissipated as heat. According to the Landau-Zener transition probability (42), any momentum that builds along the isomerization coordinate enhances the coupling efficiency to the ground-state surface on the 13-*cis* side. Consequently, efficient isomerization requires that the retinal nuclei be able to rapidly rearrange with minimal steric hindrance by the protein. The fact that the photoisomerization efficiency exhibited in bR is substantially greater than that in disordered solvents suggests that the protein cavity surrounding retinal is quite tolerant of the nuclear rearrangement required for all-*trans* to 13-*cis* isomerization.

The overall isomerization rate need not be fast to be efficient. According to the gap law, radiationless transitions become important after surmounting the barrier along the isomerization coordinate. Con-

sequently, mutations that elevate the height of the barrier will slow the overall isomerization reaction but need not compromise its efficiency, as has been observed (25, 43). In contrast, mutations or retinal analogs that contribute additional steric hindrance along the isomerization coordinate would surely decrease the photoisomerization efficiency.

### Further Complications: Nonexponential Chemical Dynamics

Despite the apparent success of the three-state model, recent experiments have revealed complications that require further extensions to the model. For example, the decay of the excited-state population is poorly described by the 0.5-ps exponential time constant reported elsewhere (30–32, 43, 44) but is modeled reasonably well by two or three exponential terms (35, 45). Given the complication of nonexponential dynamics, efforts to obtain a fundamental understanding of chemical dynamics in bR might appear to be hopeless. Whether or not that is true depends on our ability to account for the origin of the nonexponential dynamics.

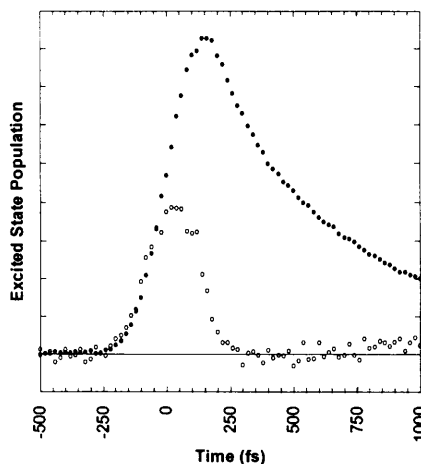


**Fig. 4.** Time-dependent decay of the excited states of all-*trans* retinal (bR\*; filled circles) and 13-*cis* retinal (K\*; open circles), the first stable photoproduct. The bR\* dynamics were measured by photoexciting the sample at 17,000 cm<sup>-1</sup> and probing the excited-state population at 10,000 cm<sup>-1</sup>. To measure the K\* dynamics, the K state was first prepared by photoexciting a bR sample at 19,120 cm<sup>-1</sup> with a 5-ns pulse from a frequency-doubled Nd:YLiF<sub>4</sub> laser. After a 10-ns delay, the resulting mixture of bR and K was photoexcited at their isosbestic point (17,000 cm<sup>-1</sup>) with a femtosecond laser pulse. The time-dependence of the excited-state population was again probed at 10,000 cm<sup>-1</sup>. To recover the K\*-only dynamics, the contribution from bR\* was estimated and subtracted, and the amplitude of the resulting curve was normalized relative to the bR\*-only dynamics.

A triexponential decay might be interpreted in terms of three identifiable species, each decaying with its own unique rate. If there are three unique species, they should be distinguishable through their absorbance or emission spectra, or both. For example, if multiple species are distinguishable in absorbance, a change in the excitation wavelength will alter the probability of exciting each species, and the relative amplitudes of the three decay components will vary with excitation wavelength. If multiple species are distinguishable in emission, the stimulated emission contribution to the time-resolved absorbance spectrum would shift in time as the fast-decaying species disappears and the slow-decaying species persists. Neither of these predictions is realized: the relative amplitudes for the three components (Fig. 5) are the same within scatter for all excitation wavelengths explored, and the stimulated emission spectrum at 1 ps is virtually the same as that at 0.2 ps (35). If there are multiple species present in the bR sample, they are spectroscopically equivalent in both absorbance and emission.

Nonexponential dynamics could be a manifestation of the conformational heterogeneity that arises from thermally driven transitions among the conformational substates accessible to a protein (46). Because the protein surrounding the retinal in bR modulates its photochemical reactivity, subtle conformational differences might lead to altered reaction rates.

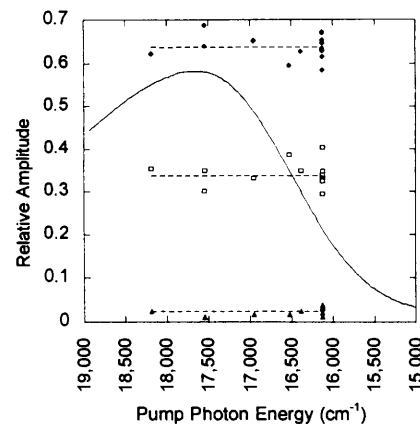


**Fig. 5.** Wavelength dependence of the triexponential amplitudes used to model the decay of the excited-state population (probed at 11,200 cm<sup>-1</sup>). The decay dynamics for 14 separate measurements spread over six wavelengths were simultaneously least-squares fitted with three globally optimized time constants. The normalized amplitudes for the fast (diamonds), intermediate (squares), and slow (triangles) components appear to be constant (dashed lines) over this range of pump wavelengths. The global time constants were 0.24, 0.74, and 8.5 ps, respectively. For comparison, a scaled equilibrium absorbance spectrum of bR (solid line) is shown.

Therefore, nonexponential dynamics can conceivably arise from a distribution of rates. To test this proposal, we modeled the time-dependent decay of the excited-state population with a distribution of rates, with the resulting distribution subject to only one constraint: the model must give the best fit possible while maximizing entropy (Fig. 6). The entropy referred to in this maximum-entropy method (MEM) (47) is proportional to  $-\sum_i p_i (\ln p_i)$ , where  $p_i$  is the probability that the protein is in state  $i$  and reacts with a rate constant  $k_i$ . The time-dependent decay of the excited-state population is then described by  $\sum_i p_i \exp(-k_i t)$ . Accordingly, two substates with similar rates are preferred to one substate, providing a driving force to broaden the distribution to the maximum extent possible without compromising the quality of the fit. Remarkably, the best fit distribution obtained with the use of MEM (Fig. 6) is not a single broad distribution, as might have been expected. Rather, the distribution has two well-defined and narrow features centered near 0.24 and 0.75 ps, whose integrated amplitudes are approxi-

mately 2:1. Because the amplitude of the small feature near 10 ps increases with sample age and light exposure, it likely corresponds to a degraded by-product of bR. The time constants and amplitudes associated with the two main MEM features are similar to the parameters obtained when the same data are modeled with a triexponential function. Moreover, these parameters are similar to those reported by time-resolved fluorescence emission (45), whose average between 770 and 900 nm was found to be 0.21 and 0.79 ps with a 1.8:1 ratio. Consequently, there are two fundamental time constants involved in the excited-state relaxation of retinal in bR (48).

Dobler *et al.* (32) reported a 0.2-ps growth of the transient absorbance in the vicinity of the photoproduct absorbance. Because a 0.2-ps process is faster than the purported 0.5-ps decay of the state that necessarily precedes the formation of photoproduct, they assigned the 0.2-ps process to nuclear motion along the photoisomerization coordinate and away from the Franck-Condon active region. Given the

MEM analysis reported here and the static nature of the stimulated emission spectrum on the 0.2-ps time scale (35, 36), it now appears that the 0.2-ps growth of the transient absorbance corresponds to the formation of photoproduct. Interestingly, the growth of photoproduct appears to be dominated by the faster of the two excited-state decay components (49). The 2:1 ratio of amplitudes invites an interesting comparison with the quantum efficiency for photoisomerization. If the dominant pathway produces photoproduct and the minor pathway does not, a 2:1 partitioning along these two pathways would lead to a quantum efficiency of  $2/(1+2) = 0.67$ , a result similar to the reported value of about 0.64 (21). Evidently, more than one species and pathway needs to be invoked to account for the two dominant time constants exhibited in the chemical dynamics of photoexcited bR. Further work is needed to develop a detailed reaction scheme that is physically reasonable and consistent with known, reliable data. It appears ever more promising that the chemical dynamics of a process as complex as the isomerization of retinal in bR may be elucidated at a high level of mechanistic detail.

## Conclusions

Chemical dynamics in the condensed phase cannot be probed at the same level of detail as small molecules in the gas phase. Nevertheless, using advanced ultrafast spectroscopic techniques, one can still learn much about chemical dynamics in the condensed phase, particularly for proteins and enzymes whose selectivity and efficiency leads to one dominant photoreaction pathway. The mechanistic insights gained by such studies can go far toward answering the question of how the surrounding environment modifies the reaction pathway. Furthermore, once ultrafast time-resolved protein crystallography becomes a reality, the complement of optical and x-ray methods should lead to the mechanistic insights required for the rational design of proteins and ligands with tailored function.

## REFERENCES AND NOTES

1. V. Šrajer *et al.*, *Science* **274**, 1726 (1996); B. Perman *et al.*, *ibid.* **279**, 1946 (1998).
2. A joint collaboration among P. A. Anfinsen, K. Moffat, G. N. Phillips Jr., and M. Wulff was established to investigate ligand docking sites and pathways in myoglobin with 100-ps time resolution.
3. Brilliance refers to the x-ray flux that can be delivered to a small sample that is distant from the source. All other things equal, sources with smaller dimensions, smaller divergence, or larger flux have greater brilliance.
4. R. W. Schoenlein *et al.*, *Science* **274**, 236 (1996); C. Rischel *et al.*, *Nature* **390**, 490 (1997).
5. R. R. Birge, *Sci. Am.* **272** (no. 3), 90 (1995).

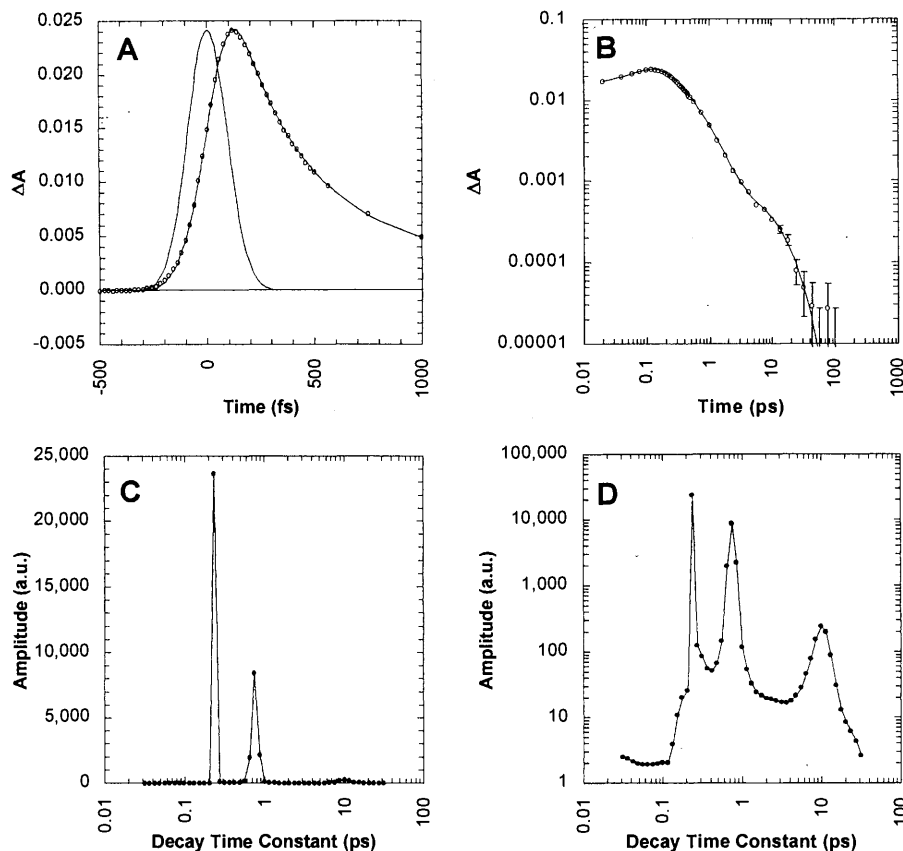


**Fig. 6.** The decay of the excited-state population (probed at  $11,200\text{ cm}^{-1}$ ) was modeled with a distribution of rates using MEM. **(A)** Linear plot of the decay (open circles), fitted with MEM (line). The instrument response function (Gaussian curve) is also shown. **(B)** Logarithmic plot of the same decay. **(C)** Linear plot of MEM amplitudes (in arbitrary units) versus rates. **(D)** Logarithmic plot of MEM amplitudes versus rates. The distribution reveals sharp peaks at 0.24 and 0.75 ps. A small, broad peak is also apparent near 10 ps.



6. Y. Kimura *et al.*, *Nature* **389**, 206 (1997); N. Grigorieff, T. A. Ceska, K. H. Downing, J. M. Baldwin, R. Henderson, *J. Mol. Biol.* **259**, 393 (1996).
7. E. Pebay-Peyroula, G. Rummel, J. P. Rosenbusch, E. M. Landau, *Science* **277**, 1676 (1997).
8. L. Song, M. A. El-Sayed, J. K. Lanyi, *ibid.* **261**, 891 (1993).
9. S. L. Logunov, L. Song, M. A. El-Sayed, *J. Phys. Chem.* **100**, 18586 (1996).
10. Q. Zhong *et al.*, *J. Am. Chem. Soc.* **118**, 12828 (1996).
11. J. K. Delaney *et al.*, *Proc. Natl. Acad. Sci. U.S.A.* **92**, 2101 (1995); J. K. Delaney *et al.*, *J. Phys. Chem.* **97**, 12416 (1993).
12. R. W. Schoenlein *et al.*, *Science* **254**, 412 (1991); T. Kobayashi *et al.*, *J. Phys. Chem. B* **102**, 272 (1998); H. Kandori *et al.*, *Chem. Phys. Lett.* **211**, 385 (1993); T. Arit, S. Schmidt, W. Zinth, U. Haupts, D. Oesterhelt, *ibid.* **241**, 559 (1995).
13. D. Oesterhelt and W. Stoerkenius, *Nature New Biol.* **233**, 149 (1971).
14. E. Racker and W. Stoerkenius, *J. Biol. Chem.* **249**, 662 (1974).
15. Retinal also functions as the visual pigment in rhodopsin, where it photoisomerizes from its 11-*cis* form to its all-*trans* form and triggers a visual response.
16. A. Lewis *et al.*, *Proc. Natl. Acad. Sci. U.S.A.* **71**, 4462 (1974); N. V. Katre *et al.*, *ibid.* **78**, 4068 (1981).
17. M. Braiman and R. A. Mathies, *ibid.* **79**, 403 (1982); M. J. Pettei *et al.*, *Biochemistry* **16**, 1955 (1977); S. O. Smith *et al.*, *J. Membr. Biol.* **85**, 95 (1985); S. O. Smith *et al.*, *Proc. Natl. Acad. Sci. U.S.A.* **83**, 967 (1986).
18. K. Gerwert, B. Hess, J. Soppa, D. Oesterhelt, *Proc. Natl. Acad. Sci. U.S.A.* **86**, 4943 (1989); M. S. Braiman *et al.*, *Biochemistry* **27**, 8516 (1988).
19. Y. Koyama *et al.*, *Photochem. Photobiol.* **54**, 433 (1991).
20. M. G. Motto, M. Sheves, K. Tsujimoto, V. Balogh-Nair, K. Nakanishi, *J. Am. Chem. Soc.* **102**, 7947 (1980); K. Nakanishi *et al.*, *ibid.*, p. 7945.
21. R. Govindjee *et al.*, *Biophys. J.* **58**, 597 (1990); M. Rohr *et al.*, *J. Phys. Chem.* **96**, 6055 (1992); L. Song *et al.*, *ibid.* **100**, 10479 (1996).
22. M. A. El-Sayed and S. Logunov, *Pure Appl. Chem.* **69**, 749 (1997).
23. J. K. Lanyi, *J. Biol. Chem.* **272**, 31209 (1997).
24. R. R. Birge *et al.*, *J. Am. Chem. Soc.* **113**, 4327 (1991).
25. S. L. Logunov and M. A. El-Sayed, *J. Phys. Chem. B* **101**, 6629 (1997).
26. G. Varo and J. K. Lanyi, *Biochemistry* **30**, 7165 (1991).
27. The 13-*cis* form is destabilized in "light-adapted" bR, where the C=N bond of the Schiff base is maintained in the *anti* configuration; it becomes nearly as stable as all-*trans* retinal when the C=N bond "isomerizes" to its *syn* configuration. Both the all-*trans* with *anti* and the 13-*cis* with *syn* forms are populated in "dark-adapted" bR. See G. S. Harbison *et al.*, *Proc. Natl. Acad. Sci. U.S.A.* **81**, 1706 (1984).
28. K. J. Kaufmann, P. M. Rentzepis, W. Stoerkenius, A. Lewis, *Biochem. Biophys. Res. Commun.* **68**, 1109 (1976).
29. T. Althaus, W. Eisfeld, R. Lohrmann, M. Stockburger, *Isr. J. Chem.* **35**, 227 (1995); H. Hamaguchi and T. L. Gustafson, *Annu. Rev. Phys. Chem.* **45**, 593 (1994); T. L. Brack and G. H. Atkinson, *J. Phys. Chem.* **95**, 2351 (1991); S. J. Doig, P. J. Reid, R. A. Mathies, *J. Chem. Phys.* **85**, 6372 (1991); G. H. Atkinson *et al.*, *Chem. Phys.* **131**, 1 (1989).
30. J. W. Petrich *et al.*, *Chem. Phys. Lett.* **137**, 369 (1987).
31. R. A. Mathies *et al.*, *Science* **240**, 777 (1988).
32. J. Döbler, W. Zinth, W. Kaiser, D. Oesterhelt, *Chem. Phys. Lett.* **144**, 215 (1988).
33. R. R. Alfano *et al.*, *Biophys. J.* **16**, 541 (1976); S. L. Shapiro *et al.*, *ibid.* **23**, 383 (1978).
34. S. L. Dexheimer *et al.*, *Chem. Phys. Lett.* **188**, 61 (1992).
35. K. C. Hasson, F. Gai, P. A. Anfinrud, *Proc. Natl. Acad. Sci. U.S.A.* **93**, 15124 (1996).
36. F. Gai, K. C. Hasson, P. A. Anfinrud, in *Ultrafast Phenomena X*, P. F. Barbara, J. G. Fujimoto, W. H. Knox, W. Zinth, Eds. (Springer Ser. Chem. Phys. 62, Springer-Verlag, Berlin, 1996), pp. 353-354.
37. G. Haran *et al.*, *Chem. Phys. Lett.* **261**, 389 (1996).
38. F. Gai, J. C. McDonald, P. A. Anfinrud, *J. Am. Chem. Soc.* **119**, 6201 (1997).
39. K. Schulten *et al.*, *Isr. J. Chem.* **35**, 447 (1995); W. Humphrey, E. Bamberg, K. Schulten, *Biophys. J.* **72**, 1347 (1997); J. R. Tallent, J. A. Stuart, Q. W. Song, R. R. Birge, in preparation.
40. G. G. Kochendoerfer and R. A. Mathies, *Isr. J. Chem.* **35**, 211 (1995).
41. K. F. Freed, in *Radiationless Processes in Molecules and Condensed Phases*, F. K. Fong, Ed. (Springer, Berlin, 1976), pp. 23-168.
42. L. D. Landau, *Phys. Z. Sowjetunion* **2**, 46 (1932); C. Zener, *Proc. R. Soc. London Ser. A* **137**, 696 (1932).
43. S. L. Logunov, M. A. El-Sayed, J. K. Lanyi, *Biophys. J.* **70**, 2875 (1996).
44. S. L. Logunov, M. A. El-Sayed, L. Song, *J. Phys. Chem.* **100**, 2391 (1996).
45. M. Du and G. R. Fleming, *Biophys. Chem.* **48**, 101 (1993).
46. D. Beece *et al.*, *Biochemistry* **19**, 5147 (1980).
47. S. F. Gull and G. J. Daniell, *Nature* **272**, 686 (1978); P. J. Steinbach *et al.*, *Biophys. J.* **61**, 235 (1992).
48. Multiexponent kinetics are not unique to bR: the chemical dynamics of halorhodopsin (hR) have also been modeled with two to three exponential components [H. Kandori, K. Yoshihara, H. Tomioka, H. Sasabe, Y. Shichida, *Chem. Phys. Lett.* **211**, 385 (1993); T. Arit, S. Schmidt, W. Zinth, U. Haupts, D. Oesterhelt, *ibid.* **241**, 559 (1995)], although it remains to be determined whether the hR kinetics are distributed or arise from two (or more) well-defined components.
49. F. Gai, K. C. Hasson, J. C. McDonald, P. A. Anfinrud, unpublished data.
50. Experimental methods: The pump pulse was generated by frequency doubling the signal output of a home-built  $\beta$ -barium borate-based optical parametric amplifier (OPA). The probe pulse was derived from a broadband continuum that was generated by focusing the output of a second OPA into a 3-mm sapphire crystal. A regeneratively amplified Ti:sapphire laser system (Clark-MXR, Dexter, MI) generated the optical pulses (1 kHz, 0.8 mJ, 120 fs, 780 nm) that powered the two OPAs. The bR sample (Sigma) was suspended in Hepes buffer (pH 7.4) and loaded into a sample cell with a 1-mm path length.
51. This work was supported in part by National Institutes of Health grant DK45306, the Beckman Foundation, the Mitsubishi Kasei Corporation, and the National Science Foundation (Young Investigator Award to P.A.A.; Graduate Research Fellowship to J.C.M.).

# Electron Transfer: Classical Approaches and New Frontiers

Helmut Tributsch\* and Ludwig Pohlmann

Electron transfer, under conditions of weak interaction and a medium acting as a passive thermal bath, is very well understood. When electron transfer is accompanied by transient chemical bonding, such as in interfacial coordination electrochemical mechanisms, strong interaction and molecular selectivity are involved. These mechanisms, which take advantage of "passive self-organization," cannot yet be properly described theoretically, but they show substantial experimental promise for energy conversion and catalysis. The biggest challenge for the future, however, may be dynamic, self-organized electron transfer. As with other energy fluxes, a suitable positive feedback mechanism, through an active molecular environment, can lead to a (transient) decrease of entropy equivalent to an increase of molecular electronic order for the activated complex. A resulting substantial increase in the rate of electron transfer and the possibility of cooperative transfer of several electrons (without intermediates) can be deduced from phenomenological theory. The need to extend our present knowledge may be derived from the observation that chemical syntheses and fuel utilization in industry typically require high temperatures (where catalysis is less relevant), whereas corresponding processes in biological systems are catalyzed at environmental conditions. This article therefore focuses on interfacial or membrane-bound electron transfer and investigates an aspect that nature has developed to a high degree of perfection: self-organization.

Electron transfer, especially as an interfacial reaction, is a tremendously important process that controls mechanisms ranging from photosynthesis and respiration to electrochemical energy systems and corrosion. Understanding of its principles began basically in the 1940s with the transition state theory (TST) (1) and the Kramers theory

(2) describing reaction rates on a microscopic basis. According to the Kramers theory, the rate constant accounts for the "frictional" effect of the surrounding medium, the immediate chemical surrounding of the electron transfer species, and includes the TST result as an upper limit. A largely empirical concept for understanding the dependence of rate constants on thermodynamic and molecular dynamic parameters was developed in the 1950s with a subsequent justification by derivation from basic principles (3). For this accomplishment,

The authors are at the Hahn-Meitner-Institut, Department Solare Energetik, Glienecker Strasse 100, D-14109 Berlin, Germany.

\*To whom correspondence should be addressed. E-mail: Tributsch@hmi.de